Seismic reflection surveys before and after BEXAR at the Nevada Test Site

Final Report to

Los Alamos National Laboratory

on contract #9-XQO-G8575-1

by Rick Milller and Don Steeples

of the

Kansas Geological Survey

The University of Kansas

DATE: January 7, 1992

Open file Report 91-55

CONTENTS

	Page
Introduction	1
Background	1
Project	1
Discussion of Seismic Reflection Technique	2
Data Aquisition	3
Walk-away Noise Tests (P-wave)	4
Walk-away Noise Tests (S-wave)	5
Data Processing	5
Discussion	7
Line 1 P-wave Data	7
Line 2 P-wave Data	7
Other Data Recorded for this Report	10
Conclusions	11
Recommendations	11
References	13
Tables	
Table 1. Seismic Data-Processing Flow Chart	15
Table 2. Uphole Survey Near BEXAR	16
Table 3. Uphole Survey about 5 Miles from BEXAR	17
Figure Captions	18

SEISMIC REFLECTION STUDIES OF THE BEXAR SPALL ZONE

INTRODUCTION

Background

It is believed that spall may have an important effect on various DOE systems designed for verification of nuclear underground test treaties. The acoustic pulse studied by the Ionospheric Monitoring Program is created specifically by the rapid acceleration of the ground surface of the spall region. Simulation studies indicated that spall effects on surface and body waves may need to be included for proper regional discrimination and yield estimation (Taylor and Randall, 1989).

Detailed experimental studies of spall have been sparse. Some work with small contained chemical explosions (Stump, 1985) have measured the spall mass and characteristics. There is a need to extend these measurements to full UGT strengths.

Project

Shallow-depth, high-frequency seismic reflection surveys of a spall zone were conducted at the Nevada Test Site, both preceding and following BEXAR, an underground test on Pahute mesa. Two seismic lines were run in the vicinity of the expected spall zone of the underground test. Both P-wave and shear-wave sources were used on each line.

Discussion of Seismic Reflection Technique

The following paragraphs briefly introduce some of the specific difficulties associated with applying seismic reflection to non-traditional problems. Detailed knowledge of the near-surface material is often crucial in many engineering, environmental and groundwater problems. Data possessing the necessary detail for conclusive mapping of physical phenomena within 100 meters of the earth's surface have generally come from extensive drilling programs which are time consuming, expensive, and environmentally undesirable. High resolution seismic-reflection profiling has been used to image surfaces as shallow as 3 m and resolve beds as thin as 1 m in a variety of near-surface geologic settings (Schepers, 1975; Doornenbal and Helbig, 1983; Birkelo et al., 1987; Myers et al., 1987; Branham and Steeples, 1988).

Using conventional reflection techniques, shallow reflections are difficult to separate from other energy arriving in the early portions of the seismograms (Steeples and Miller, 1990). The amplitudes of these shallow-reflected waves at commonly recorded frequencies are smaller than the amplitudes of unwanted waves, particularly ground roll, refractions, and air-coupled waves. Detection of shallow-reflecting events requires closely spaced source-receiver geometries, analog low-cut filtering, a suitable high-frequency seismic source, and a seismograph with quiet amplifiers and analog/digital (A/D) conversion into a large digital word (Knapp and Steeples, 1986). These criteria allow a minimum of unwanted energy to be recorded which, in turn, allows identification of subtle shallow reflectors previously obscured using more common seismic-reflection procedures.

Typical energy sources for shallow engineering studies include sledge hammer (Hunter et al., 1981; Meidav, 1969), weight drop (Doornenbal and Helbig, 1983), and small explosive charges (Pakiser and Warrick, 1956). Under ideal conditions (water table within 1 m of ground surface, solid geophone and source ground couple, etc.), the dominant frequency generated by any shallow seismic source could exceed 100 Hz at a depth of 100 m (Miller et al., 1986). In areas where near-surface conditions are not conducive to the propagation of seismic energy, certain sources will generate comparatively higher or lower frequency and amplitude seismic energy than others (Pullan and MacAuley, 1987). Previous experience has shown surface projectile sources such as the 50 caliber rifle to be cost-effective high-frequency sources in areas with a deep water table and rough rocky terrain (Miller and Steeples, 1986; Treadway et al., 1988).

The resolving potential of seismic-reflection data depends on dominant frequency (wavelength), surface station spacing, timing accuracy, and accuracy of calculated average velocities. Dominant frequencies of between 40 and 60 Hz were recorded at the NTS.

DATA ACQUISITION

Data for this study were acquired on an EG&G Geometrics 2401 seismograph. The seismograph amplifies, filters (analog), digitizes the signal into a 15-bit word, and stores the digital information in a demultiplexed format. The analog filters have a 18 dB/octave rolloff from the indicated -3 dB points. The P-wave production lines were acquired with analog low-cut filters out and 250 Hz analog high-cut filters. The 0.5 ms sampling interval selected for the production P-wave data acquisition resulted in a record length of 512 ms. The S-wave production lines were acquired with no analog low-cut filters and 250 Hz analog high-cut filters. The 1 ms sampling interval selected for the S-wave production line resulted in a record length of 1024 ms. The dynamic range of the seismograph was adequate to record P-wave reflection information at some locations.

Walk-away Noise Tests (P-wave)

The production seismic profiles were preceded by an extensive series of tests. Proper matching of analog filters for the acoustic characteristics and targets at this site allowed optimal use of the seismograph's dynamic range. Source-to-receiver offsets for walkaways ranged from 5 to 245 m with receivers spaced at 5 m. All coherent arrivals identified on walkaway data were analyzed and interpreted. All aspects of the testing were instrumental in fine-tuning the acquisition parameters and equipment used during the CDP production portion of this study.

The P-wave production data were acquired using a silenced .50-caliber seismic gun and 3-40 Hz geophones spread evenly along a 1 m in-line array. The source-to-near offset, as determined by the walkaway-noise testing, was 5 m with a source-to-far offset of 120 m. The near-surface environment prohibited the use of the downhole .50 caliber which was the source of choice at this site. Both lines 1 and 2 for trip 1 (before BEXAR detonation) and trip 2 (after BEXAR detonation) were recorded with identical parameters and equipment.

Walkaway-noise tests (S-wave)

An extensive series of walkaway noise tests was performed prior to the acquisition of the production S-wave data. The source-to-receiver offsets for the S-wave testing ranged from 5 to 245 m with receivers spaced at 5 m. Identification of coherent events and arrivals were difficult at this site due to the low levels of recorded energy. The optimization of field parameters and equipment from walkaway tests was complicated by the extremely poor acoustic properties of the near-surface.

The S-wave production data were acquired using a small block of wood with steel plates on the ends and base spikes to improve the coupling. Single 40 Hz horizontal geophones oriented perpendicular to the line were used to record the SH component of the translational wave. The source-to-nearest-receiver offset, as determined by walkaway tests, was 20 m with the source-to-farthest offset at 135 m. Two shots were recorded at each location—one with the impact direction east to west and the other with the impact direction west to east. The polarized nature of S-wave energy represented potential for enhancement techniques during processing. The acquisition parameters and equipment were identical for lines 1 and 2, both before and after detonation.

DATA PROCESSING

Data processing was done on an Intel 80486-based microcomputer using a proprietary set of algorithms (Eavesdropper) developed by the Kansas Geological Survey (Somanas et al, 1987). The processing flow was similar to those used in petroleum exploration. The main distinctions relate to precision required during velocity analysis, extra care during muting operations, and lack of deconvolution.

A conservative application (1 ms maximum shift, about 1/12 of a wavelength) of correlation statics was used to improve the coherency of interpreted reflection. Correlation statics used without restriction would produce static corrections not consistent for the two different data sets (i.e., before detonation versus after detonation).

The processing flows were held as consistent as possible so direct comparisons of data collected before the detonation could be made with data collected after detonation. The use of processes such as deconvolution and unrestricted correlation statics would not have operated consistently on the two data sets. This is also true of digital filtering. Therefore, parameters or processes that could produce data-set dependent corrections or results were not used.

The east-to-west and west-to-east components of the S-wave data from each line were initially processed independently. Then the polarity of the west-to-east component was reversed and added to the east-to-west component and CDP stacked. The intention here was to enhance S-wave energy and cancel compressional wave energy.

For all CDP data, a CDP divisor of two has been used to improve the apparent fold and increase the signal-to-noise ratio. The effect of increasing the CDP divisor from its default value of one is to gather two adjacent subsurface points together into a "CDP array". This contributed to the improved S/N and allowed the coherent stacking of the reflections on P-wave line 2.

DISCUSSION

The results of the P-wave experiments are promising as discussed below, particularly on line 2. The S-wave experiments did not produce positive results.

Line 1 P-wave data

Figure 2 is a pseudo 24-fold stack of line 1 before detonation of BEXAR. Processing was concentrated on subtle indications of coherent events between 200 and 400 ms. Some indication of a coherent event exists at about 300 ms. The dominant frequency is no greater than about 50 Hz. The presence of 60-Hz noise is quite limited on the stacked section as a result of the effectiveness of the 60-Hz notch filter that was applied.

Figure 3 is a pseudo 24-fold stack of line 1 after detonation of BEXAR. It also possesses subtle indications of coherent events between 200 and 400 ms (as noted in Figure 2). The event suggested in Figure 2 at approximately 300 ms seems to still be present after detonation. The origin of this event is not known. The 60 Hz noise source was not present when these data were acquired, but the same 60-Hz notch filter was used for consistency purposes.

Line 2 P-wave data

Figure 5 shows stacked CDP seismic P-wave reflection data from line 2 before BEXAR, and figure 7 shows the data from the same line after BEXAR. The data before the explosion show a reflection at about 240 ms two-way traveltime. The stacking velocity suggested that this reflection comes from about 150 meters deep. The data in figure 7 show two reflections, one at about 210 ms and one at about 290 ms. Stacking velocities suggest the event at 290 ms after BEXAR is from the same 150 meter depth as the pre-BEXAR 240 ms reflection.

Data in figure 4 show an identifiable reflection at about 240 ms on field files. The data in figure 6 show identifiable reflections on post-BEXAR scaled shot gathers at times of about 210 ms and 290 ms. The data of figures 4 and 6 provide confidence that the interpreted reflections on figures 5 and 7 are genuine reflections and not processing artifacts.

In order to test the validity of the velocities for the CDP stacking process, we checked the uphole traveltimes that have been collected from nearby boreholes (see tables 2 and 3). The velocities observed in the pre-BEXAR borehole measurements are higher by about 25% than the stacking velocities that were used. The one-way travel time to a depth of 150 m at the BEXAR hole is 96 ms, which converts to a two-way predicted reflection time of 192 ms for vertical incidence. This represents an average P-wave velocity of 1625 m/s to a depth of 150 m. In contrast, the stacking velocities used were 1300 m/s before BEXAR and 1150 m/s after BEXAR.

At another well about 5 miles away, however, the velocity (Table 3) was almost the same as the stacking velocity that was used for the processing. At that well, for example, the one-way travel time to a depth of 150 meters is 128 ms, which converts to a two-way travel time of 256 ms for a reflected P-wave at vertical incidence. This represents a P-wave velocity of about 1170 m/sec. The stacking velocity used for processing was 1300 m/sec before BEXAR and 1150 m/sec after BEXAR.

Stacking velocities commonly vary by at least 10% from average velocity obtained by actual one-way traveltimes. These variations are related to the use of vertical wavepaths for the uphole survey and non-vertical raypaths for the reflection data, so that any anisotropy that is present would result in a velocity discrepancy (Hughes, 1985). Also, the wavelengths for the two types of seismic observation are often significantly different, which can cause variations in observed velocity. The point is that the stacking velocity was calculated independently of the observed uphole velocity, and the two observations are within the tolerance for errors expected for the methods. Given that the stacking velocities are similar to a well about 5 miles from BEXAR and that line 2 was almost one mile from BEXAR, we believe that the stacking velocity is reasonable. The seismic lines are topographically (and probably stratigraphically) about 60 m lower than the surface at the BEXAR location.

There are three things that give us confidence that we are dealing with genuine P-wave reflections on figures 5 and 7. First, reflections are visible on a few field files or scaled shot gathers as in figures 4 and 6. Secondly, a very conservative approach was used in processing to avoid "making data". Third, the velocities used in processing are close to velocities independently produced by borehole measurements.

Note that the new reflection at 210 ms is from a shallower depth than 150 meters, probably about 105 meters. It is possible that the new reflection represents the fracture associated with spall.

We note that the frequency is slightly higher for the post-BEXAR data than for the pre-BEXAR data. One would expect that any fracturing caused by BEXAR would cause the post-BEXAR data to have lower frequencies. It is possible that the near-surface conditions were more favorable to transmitting higher frequencies later in the winter, which could explain the higher frequencies recorded in April than in February. A brief look at spectral analysis of first arrival wavelets before and after BEXAR was inconclusive in evaluating near-surface changes.

Other data recorded for this report

The P-wave data from line 1 are not of the same quality as the data from line 2. While we do not know the exact reason for that, it is worth noting that line 1 was located very near to ground zero for a previous nuclear test. It is possible that the rock was sufficiently fractured by the previous test that P-waves were not readily propagated at the site of line 1. It is also possible that the application of the 60 Hz notch filter had deleterious effects on the line 1 data.

As mentioned earlier, the S-wave data recorded for this study were not useful. The recording bandwidth that we used was probably inappropriate for the site. With P-wave dominant frequencies of about 50 Hz, we would expect the S-wave dominant frequencies to be somewhere around 25 Hz. The only horizontal geophones available in the field had natural frequency of 40 Hz. The S-wave data are shown in figures 8 to 19 inclusive.

In the interest of looking at data quality for possible experiments at Yucca flat, a walk-away noise test was run on the flats. Figures 20-23 show reflection data from Yucca flat that suggest good quality reflections could be obtained for possible similar experiments there.

CONCLUSIONS

1. At a distance of about 1.5 km from ground zero, the common-depth-point reflection method detected reflections both before and after BEXAR was detonated.

2. At a distance of about 1.5 km from ground zero, there are substantial differences in the seismic-reflection sections when comparing data collected before BEXAR with data collected after.

3. It is not yet clear whether the before and after differences in the data are caused by the spall or whether they are related to gross fracturing and reopening of joints and bedding planes in a large volume of rock in the vicinity of the explosion.

4. The data from the seismic line at distances of about 500 meters from ground zero were contaminated with 60 Hz power-line noise before BEXAR, but the power line was absent when data were collected after BEXAR. Consequently, it is not possible to make a detailed one-to-one comparison of data collected before and after the detonation.

5. The S-wave reflection experiments did not result in the detection of reflections either before or after BEXAR. It should be noted, however, that the experiment was conducted with 40-Hz horizontal geophones. Based on the 50-Hz dominant frequency of the P-wave reflection data, it is not reasonable to expect much S-wave reflection energy above 25 Hz. Any further S-wave reflection experiments should be conducted with horizontal geophones with natural frequency somewhere in the 8-Hz to 14-Hz range.

6. A walk-away noise test at Yucca flat suggests that good quality reflection data could be obtained there for similar experiments.

RECOMMENDATIONS

1. Any further spall detection research involving reflection seismology should involve tests that are detonated at least 2-3 km away from ground zero of any previous nuclear tests.

2. The seismic energy provided by the surface .50-caliber rifle is marginal for spall-detection research. We recommend that about 1/4 pound of high explosive be placed in holes drilled about 2-3 meters deep. Experiments with 400 grain or larger black powder charges could also be fruitful.

3. Near-surface static and velocity anomalies are substantial at the NTS. To maintain coherency of wave trains on the field seismograms while improving velocity analysis, a seismograph with at least 48 channels should be employed for future experiments.

4. The possibility of success may be higher at Yucca flat than on the mesa.

5. The P-wave results were sufficiently positive relative to the S-wave results that future experiments should concentrate on the P-wave reflections rather than S-wave reflections.

ACKNOWLEDGEMENTS

This report was supported by the Source Region Program at the Los Alamos National Laboratory (LANL) for the U. S. Department of Energy under contract W-705-ENG-36. The work was performed under LANL contract #9-XQO-G8575-1 with the University of Kansas. Alan Cogbill kindly provided us with velocity logs and survey locations for the ends of the seismic lines.

REFERENCES

Birkelo, B. A., Steeples, D. W., Miller, R. D., and Sophocleous, M. S., 1987, Seismic-reflection study of a shallow aquifer during a pumping test: Ground Water, 25, 703-709.

Branham, K. L, and Steeples, D. W., 1988, Cavity detection using high resolution seismic-reflection methods: Mining Engineering, 40, 115-119.

Doornenbal, J. C., and Helbig, K., 1983, High-resolution reflection seismics on a tidal flat in the Dutch Delta-acquisition, processing, and interpretation: First Break, May, 9-20.

Hughes, D. R., 1985, V w/o T (Velocity without tears): The Leading Edge, v 4, February, 50-52.

Hunter, J. A., Burns, R. A., and Good, R. L., 1981, Optimum field techniques for bedrock mapping with the multichannel engineering seismograph [Abs.]: Geophysics, 46, 451.

Hunter, J. A., Pullan S. E., Burns, R. A., Gagne, R. M., and Good, R. L., 1984, Shallow seismic-reflection mapping of the overburden-bedrock interface with the engineering seismograph--some simple techniques: Geophysics, 49, 1381-1385.

Knapp, R. W., Steeples, D. W., 1986, High resolution common depth point seismic-reflection profiling, field acquisition parameter design: Geophysics, 51, 283-294.

Meidav, T., 1969, Hammer reflection seismics in engineering geophysics: Geophysics, 34, 383-395.

Miller, R. D., Pullan, S. E., Waldner, J. S., and Haeni, F.P., 1986, Field comparison of shallow seismic sources: Geophysics, 51, 1067-1092.

Miller, R. D., and Steeples, D. W., 1986, Shallow structure from a seismic-reflection profile across the Borah Peak, Idaho, fault scarp: Geophysical Research Letters, 13, 953-956.

Myers, P. B., Miller, R. D, and Steeples, D. W., 1987, Shallow seismic-reflection profile of the Meers fault, Comanche County, Oklahoma: Geophysical Research Letters, 14, 749-752.

Pakiser, L., and Warrick, R., 1956, A preliminary evaluation of the shallow reflection seismograph: Geophysics, 21, 388-405.

Pullan, S. E., and Hunter, J. A., 1985, Seismic model studies of the overburden-bedrock reflection: Geophysics 50, 1684-1688.

Pullan, S. E., and MacAulay, H. A., 1987, An in-hole shotgun source for engineering seismic surveys: Geophysics, 52, 985-996.

Schepers, R., 1975, A seismic-reflection method for solving engineering problems: Jour. of Geophysics, 41, 367-384.

Somanas, D., Bennett, B., and Chung, Y., 1987, In-field seismic CDP processing with a microcomputer: The Leading Edge, v. 6, p. 24-26, July.

Steeples, D. W., and Knapp, R. W., 1982, Reflections from 25 feet or less; in Technical Program Abstracts and Biographies [Exp. Abs.]: Soc. Explor. Geophys. 52nd Ann. Mtg., 469-471.

Steeples, D. W., and Miller, R. D., 1990, Seismic-reflection methods applied to engineering, environmental, and ground-water problems: Soc. Explor. Geophys. volumes on Geotechnical and Environmental Geophysics, Stan Ward, ed., Volume 1: Review and Tutorial, p. 1-30.

Stump, B. W., 1985, Constraints on explosive sources with spall from near-source wave forms, Bull. Seismol. Soc. Amer., 75, 361-377.

Taylor, S. R., and G. E. Randall, 1989, The effects of spall on regional seismograms, Geophysical Research Letters, 16, 211-214.

Treadway, J. A., Steeples, D. W., and Miller, R. D., 1988, Shallow seismic study of a fault scarp near Borah Peak, Idaho: Journal of Geophysical Research, 93, 6325-6337.

Widess, W. B., 1973, How thin is a thin bed?: Geophysics, 38, 1176-1180.

TABLE 1.

SEISMIC DATA-PROCESSING FLOW CHART

1) Bad trace edit
2) Elevation statics
3) First-arrival mute
4) Spectral analysis
5) 2nd zero crossing auto-predictive deconvolution
6) Common Depth Point (CDP) sort
7) Velocity analysis
8) Surface-consistent statics
9) Bandpass filter
10) Automatic Gain Control (AGC) scale
11) Common Depth Point (CDP) stack

TABLE 2

UPHOLE SURVEY NEAR BEXAR

PROVIDED BY LANL

DEPTH (ft)	ONE-WAY TRAVELTIME (ms)
100.00	31.80
150.00	43.30
200.00	48.30
250.00	61.70
300.00	69.30
350.00	76.00
400.00	84.40
450.00	91.80
500.00	96.60
550.00	105.80
600.00	113.40
650.00	119.60
700.00	126.70
750.00	132.80
800.00	139.90
850.00	147.00
900.00	153.10
950.00	157.10
1000.00	163.20
1050.00	171.20
1100.00	177.30
1150.00	180.30
1210.00	187.90
1300.00	202.90
1350.00	210.40
1400.00	216.50
1450.00	219.50
1500.00	228.00
1550.00	231.50
1600.00	237.50
1650.00	244.60
1750.00	255.60
1800.00	258.60
1850.00	261.60
1890.00	265.60
1950.00	274.60

TABLE 3

UPHOLE SURVEY NEAR BEXAR

PROVIDED BY LANL

DEPTH (ft)	ONE-WAY TRAVELTIME (ms)
100.00	38.50
150.00	52.60
200.00	68.70
250.00	82.40
300.00	92.20
350.00	102.70
400.00	112.00
450.00	121.30
500.00	128.50
550.00	136.70
600.00	143.80
650.00	152.90
700.00	160.00
750.00	166.10
800.00	172.10
850.00	177.20
900.00	182.20
950.00	189.30
1000.00	197.30
1050.00	202.30
1100.00	208.40
1150.00	213.40
1200.00	220.40
1250.00	226.30
1300.00	230.50
1350.00	235.30
1400.00	242.60
1450.00	248.60
1500.00	255.50
1550.00	260.70
1600.00	266.50
1650.00	272.60
1700.00	277.90
1750.00	282.90
1785.00	286.60
1880.00	298.60
2070.00	316.90

FIGURE CAPTIONS

FIGURE 1. Site map showing roads and seismic line locations relative to BEXAR.

FIGURE 2. The pseudo 24-fold stack of line 1 before detonation of BEXAR with processing concentrated on subtle indications of coherent events between 200 and 400 ms. Some indication of a coherent event exists at about 300 ms. The dominant frequency is no greater than about 50 Hz. The presence of 60-Hz noise is quite limited on the stacked section as a result of the effectiveness of the 60-Hz notch.

FIGURE 3. This pseudo 24-fold stack of line 1 after detonation of BEXAR also possesses subtle indications of coherent events between 200 and 400 ms (as noted in Figure 2). The event suggested in Figure 2 at approximately 300 ms seems to still be present after detonation. The origin of this event is not known. The 60 Hz noise source was not present when this data was acquired, but the same 60-Hz notch was used on this data for consistency purposes.

FIGURE 4. The data acquired on line 2 were of superior quality and possessed a reflection interpretable on field files. The files from left to right are examples of (1) raw field file, (2) filtered, scaled, first-arrival muted, and bad-traced edited field file, (3) secondary muting to remove a non-reflection coherent wave train field file, and (4) a moved out and 2-ms static shifted field file.

FIGURE 5. Pseudo 24-fold CDP stacked seismic section from line 2 before detonation. The coherent event at 250 ms is easily interpretable. The dominant frequency is approximately 50 Hz.

FIGURE 6. Example field files from line 2 after BEXAR. These scaled shot gathers have identifiable reflections at about 210 and 290 ms.

FIGURE 7. Pseudo 24-fold CDP stacked seismic section from line 2 after detonation. There appear to be two coherent events at unique times in comparison to before detonation. The velocity is 200 ms slower after detonation, which suggests the event at 300 ms on this section is at an equivalent depth as the event at 250 ms on the before BEXAR section (Figure 5).

FIGURE 8. **NOTE: Figures 8 to 19 are S-wave CDP stacks.** Line 1 before detonation with east/west (E/W) combined with west/east (W/E).

FIGURE 9. Line 1 before detonation, E/W polarized.

FIGURE 10. Line 1 before detonation, W/E polarized.

FIGURE 11. Line 2 before detonation with E/W combined with W/E.

FIGURE 12. Line 2 before detonation, E/W polarized.

FIGURE 13. Line 2 before detonation, W/E polarized.

FIGURE 14. Line 1 after detonation with E/W combined with W/E.

FIGURE 15. Line 1 after detonation, E/W polarized.

FIGURE 16. Line 1 after detonation, W/E polarized.

FIGURE 17. Line 2 after detonation with E/W combined with W/E.

FIGURE 18. Line 2 after detonation, E/W polarized.

FIGURE 19. Line 2 after detonation, W/E polarized.

FIGURE 20. Walkaway-noise test from Yucca flat using 100 Hz analog low-cut filtering. Two events are interpretable—one at approximately 150 ms and the second at approximately 300 ms. Both events possess the characteristic appearance and geometric shape of reflections.

FIGURE 21. Walkaway-noise test from same location as Figure 20 using a 50-Hz analog low-cut filter.

FIGURE 22. 100 Hz digital low cut on walkaway data from Figure 20.

FIGURE 23. 100 Hz digital low cut on walkaway data from Figure 21.

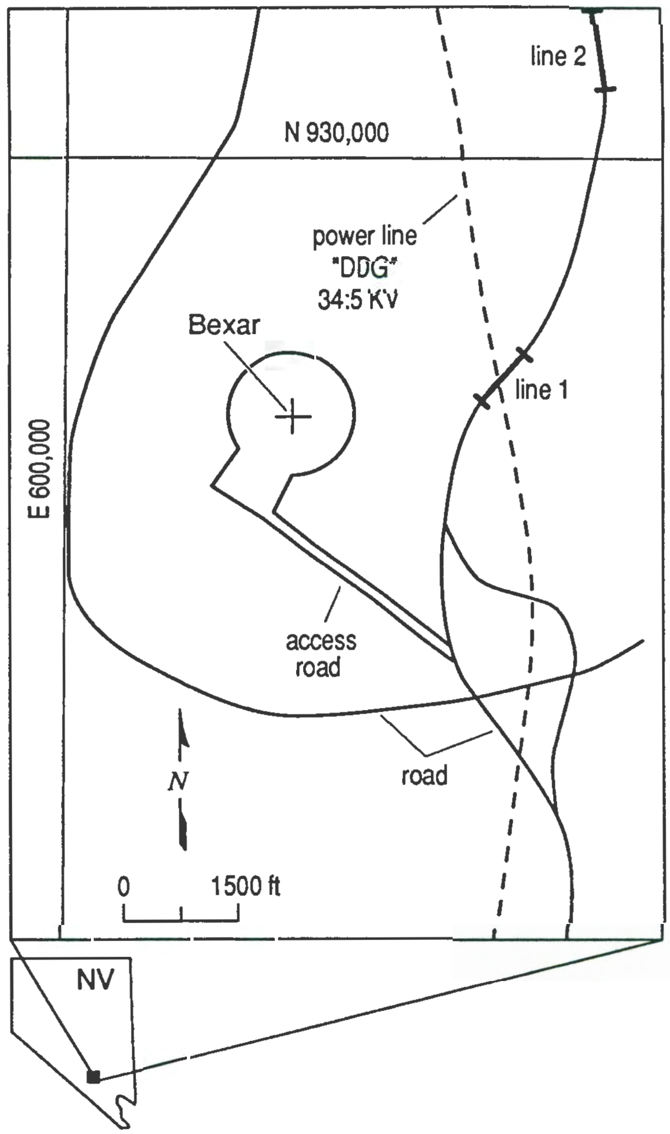

Line ends (Nevada Coordiate System)

Line 1: N 927, 102 ; E 605, 421
N 927, 640 ; E 605, 786

Line 2: N 930, 809 ; E 606, 606
N 931, 791 ; E 606, 481

fig 1. Site map at Nevada Test Site.

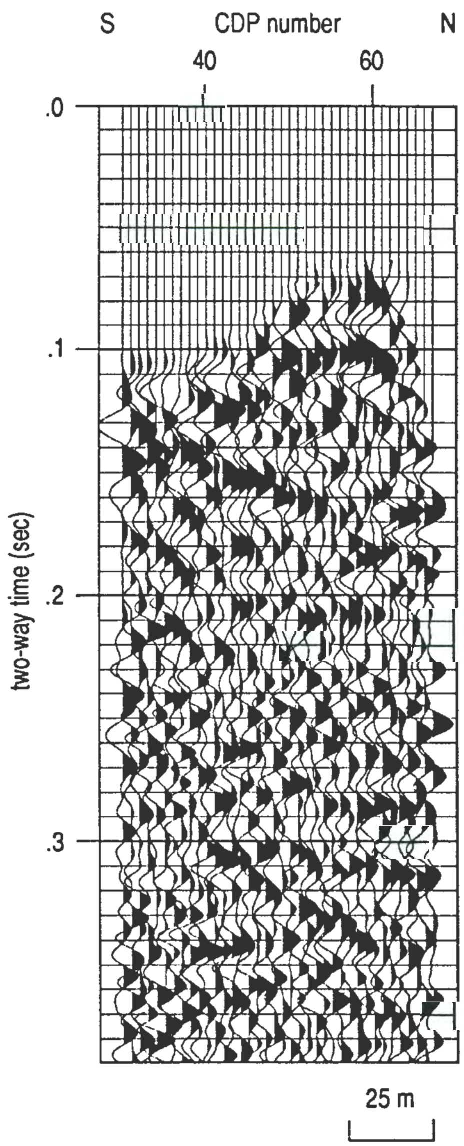

fig 2

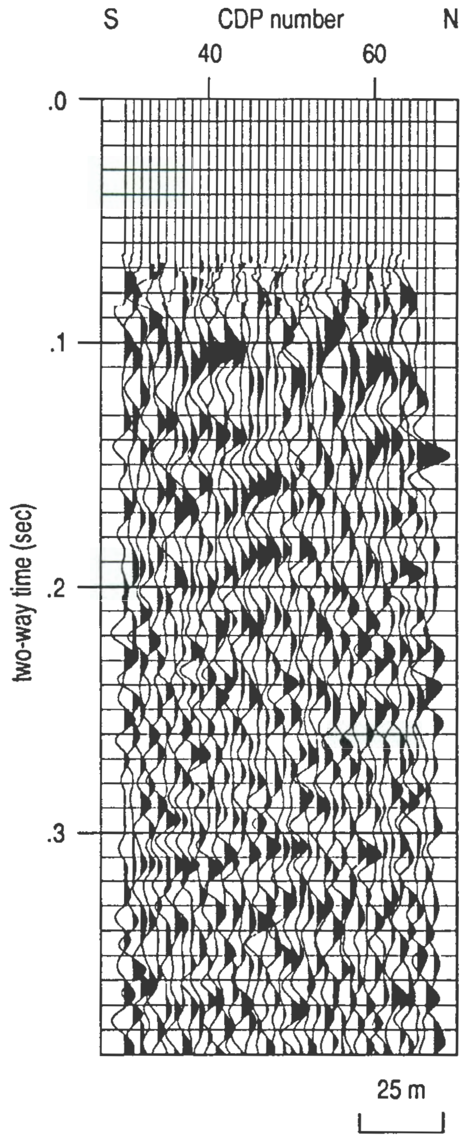

fig 3

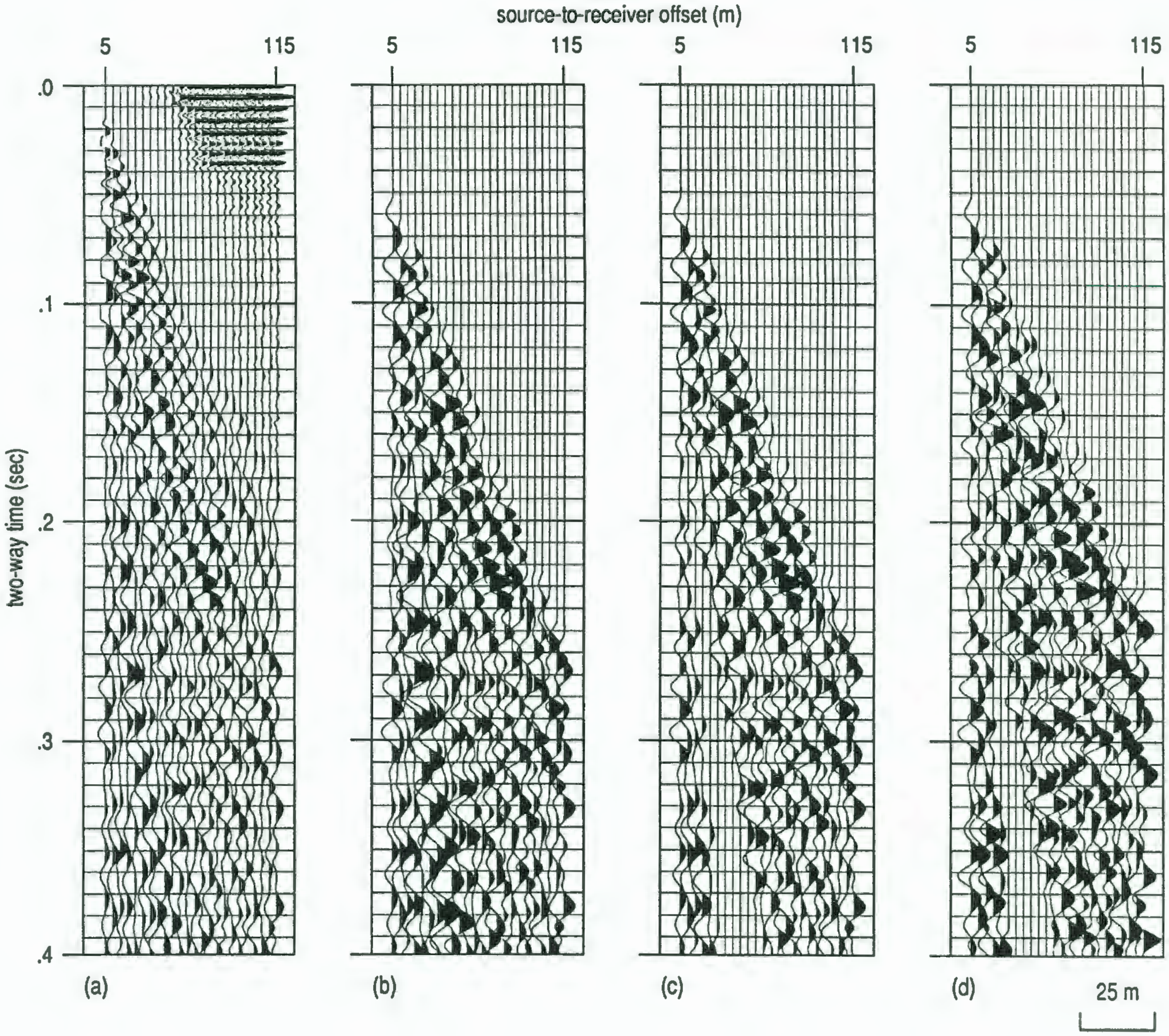
source-to-receiver offset (m)
5
115
two-way time (sec)
.0
.1
.2
.3
.4
(a)
(b)
(c)
(d)
25 m

fig 4

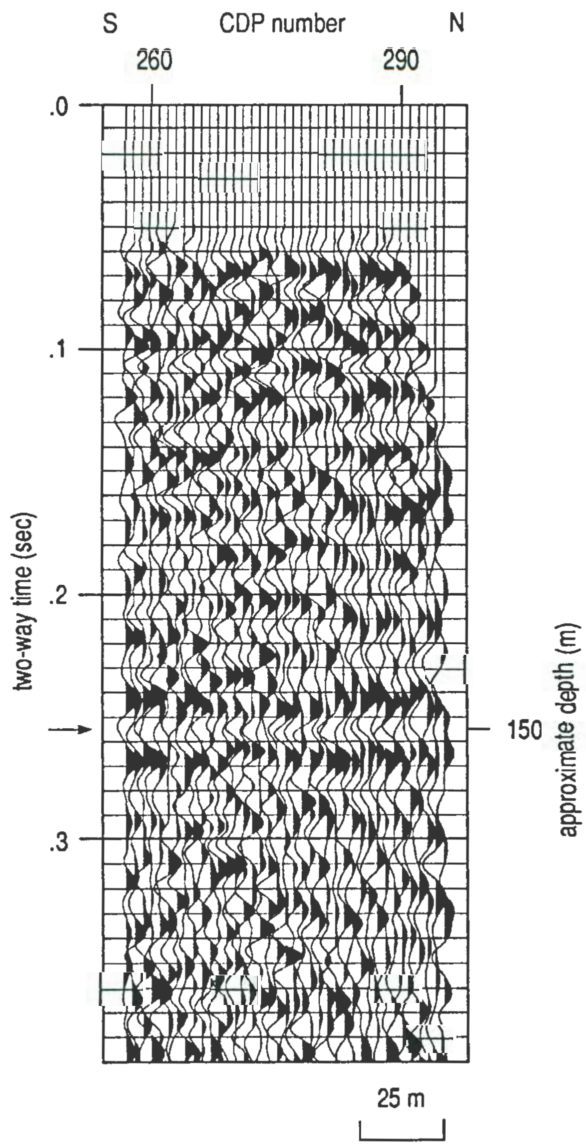
S
CDP number
N
260
290
.0
.1
.2
.3
two-way time (sec)
150
approximate depth (m)
25 m

fig 5

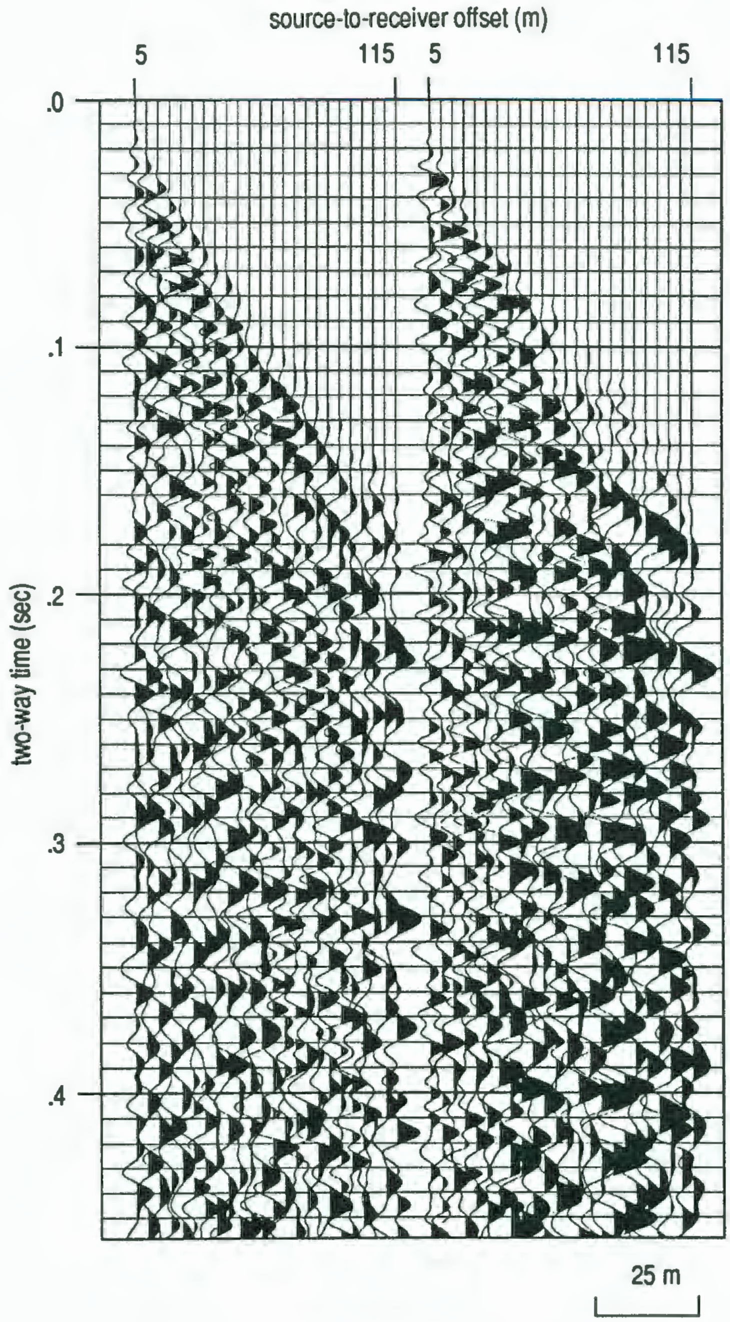

source-to-receiver offset (m)
5
115
5
115
.0
.1
.2
.3
.4
two-way time (sec)
25 m

fig 6

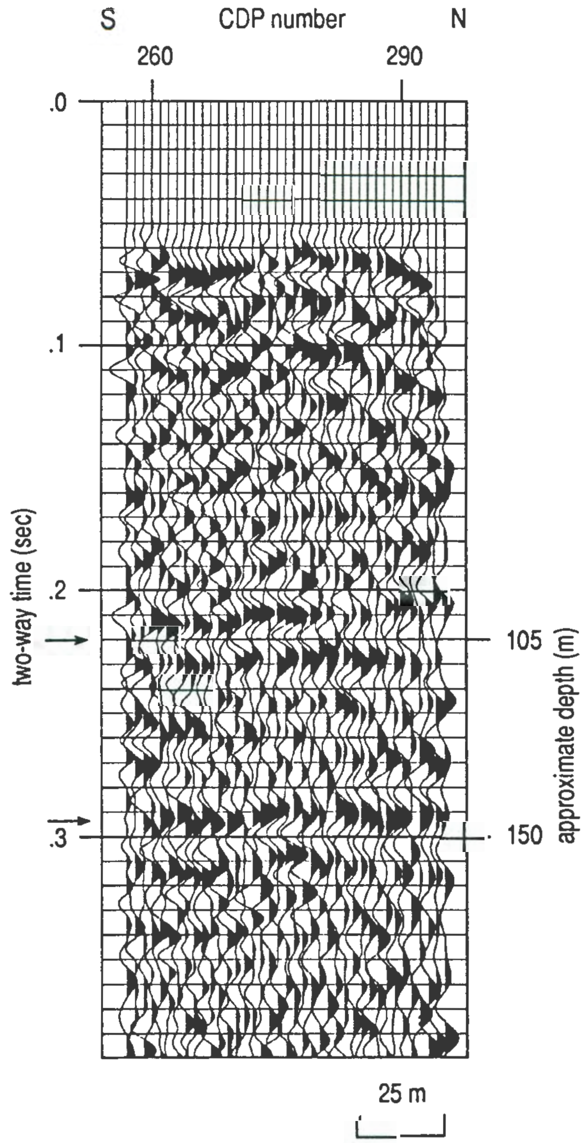
S
CDP number
N
260
290
.0
.1
.2
.3
two-way time (sec)
105
150
approximate depth (m)
25 m

fig 7

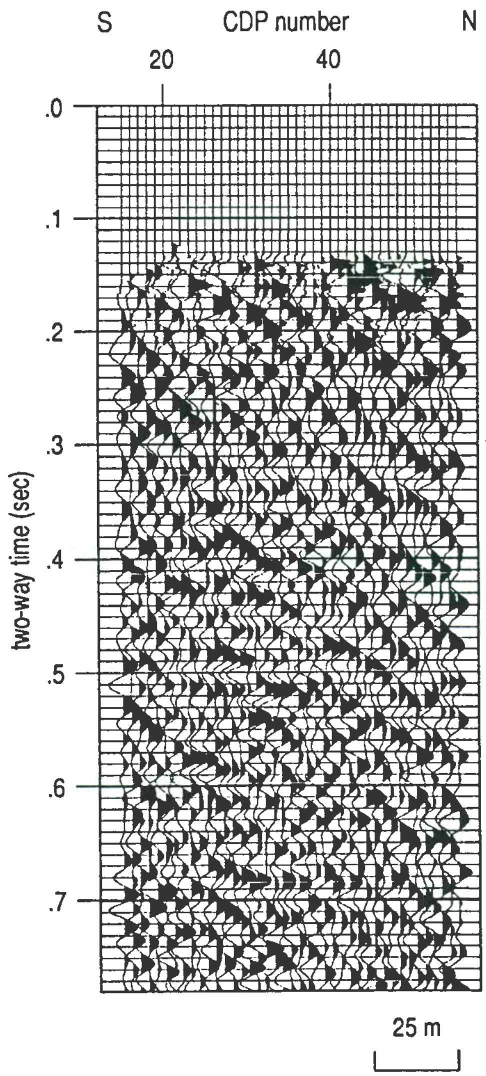

fig 8

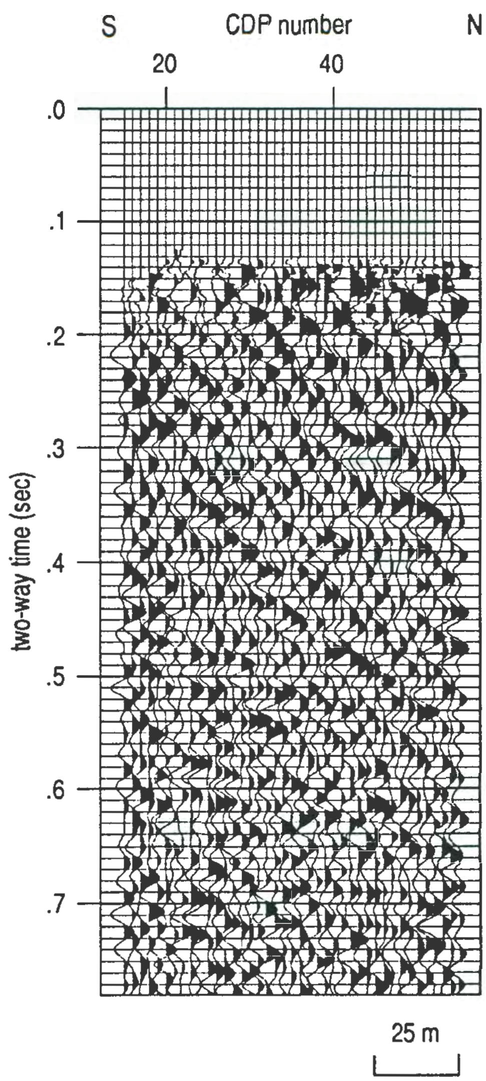

fig 9

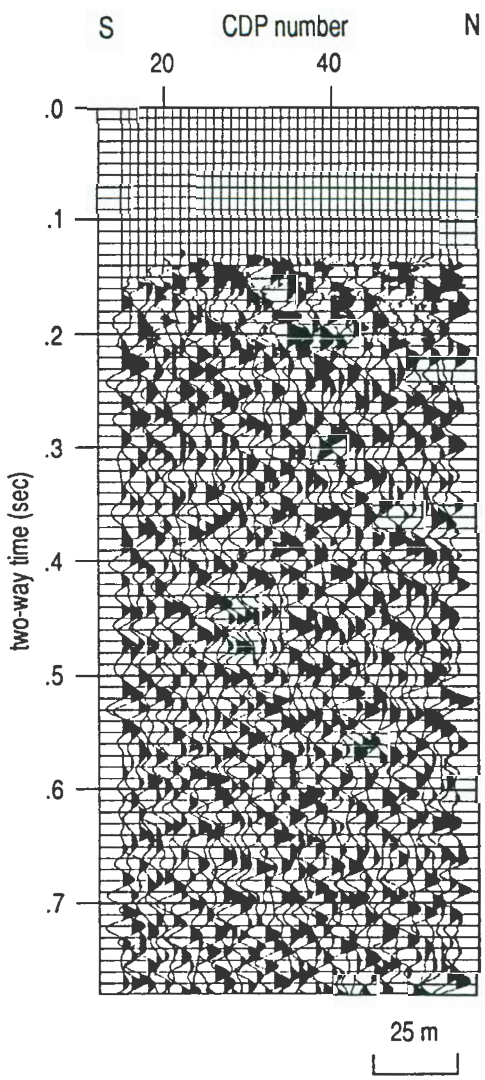

fig 10

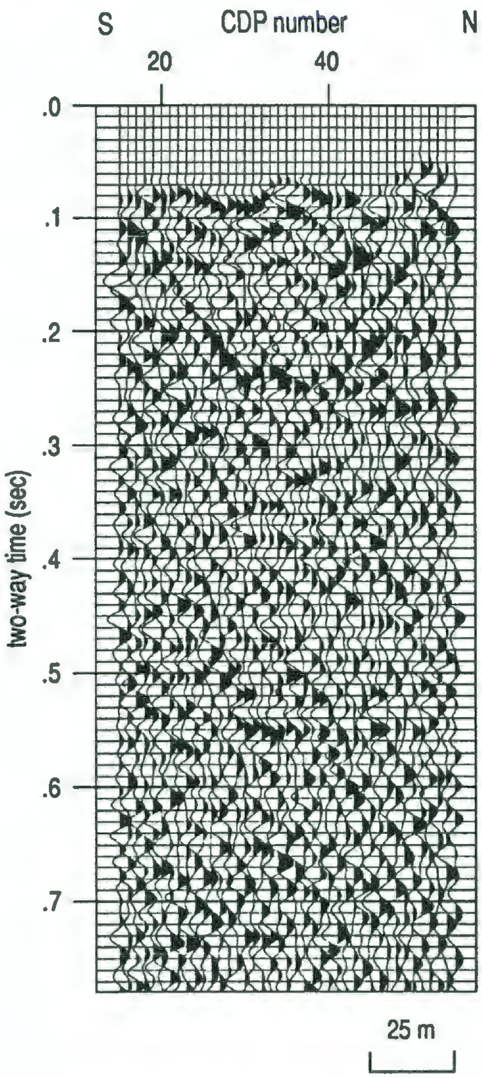

fig 11

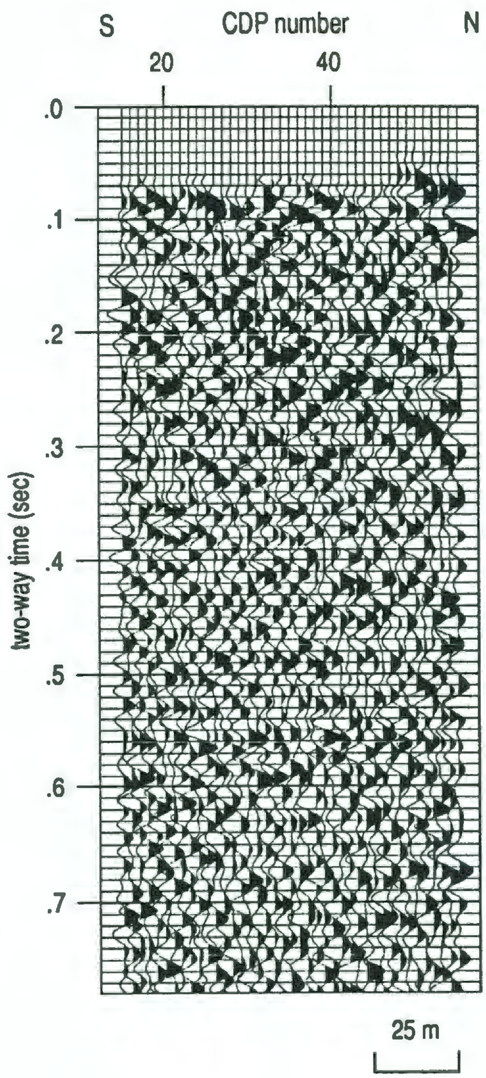

fig 12

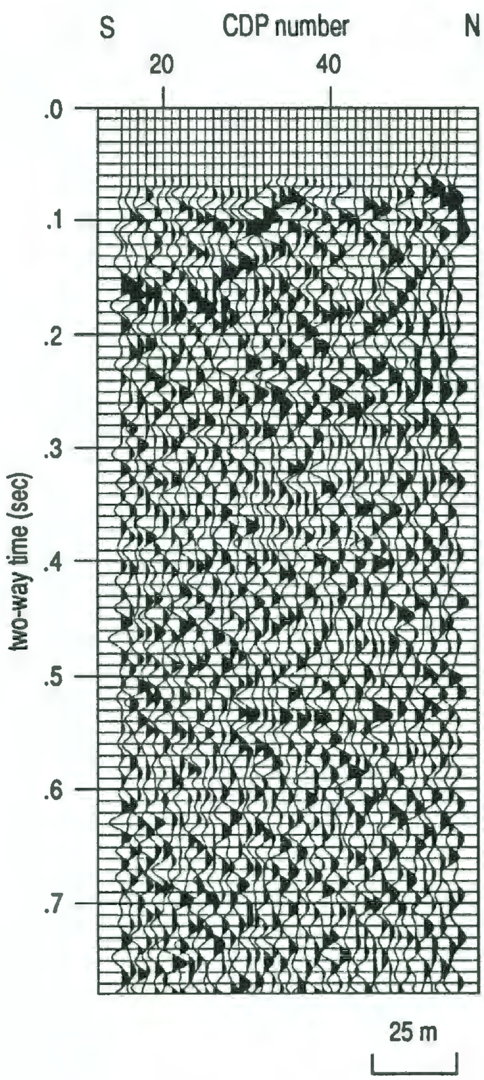

fig 13

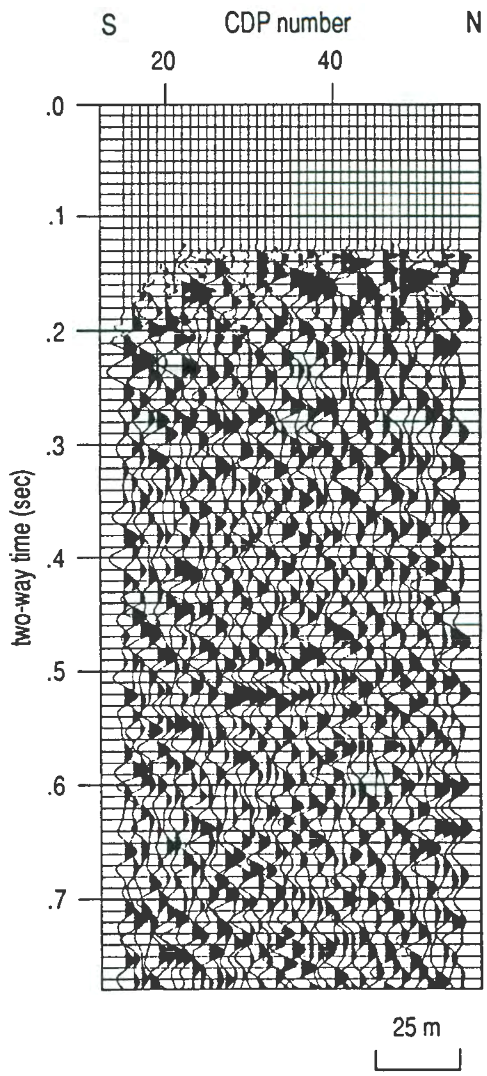

fig 14

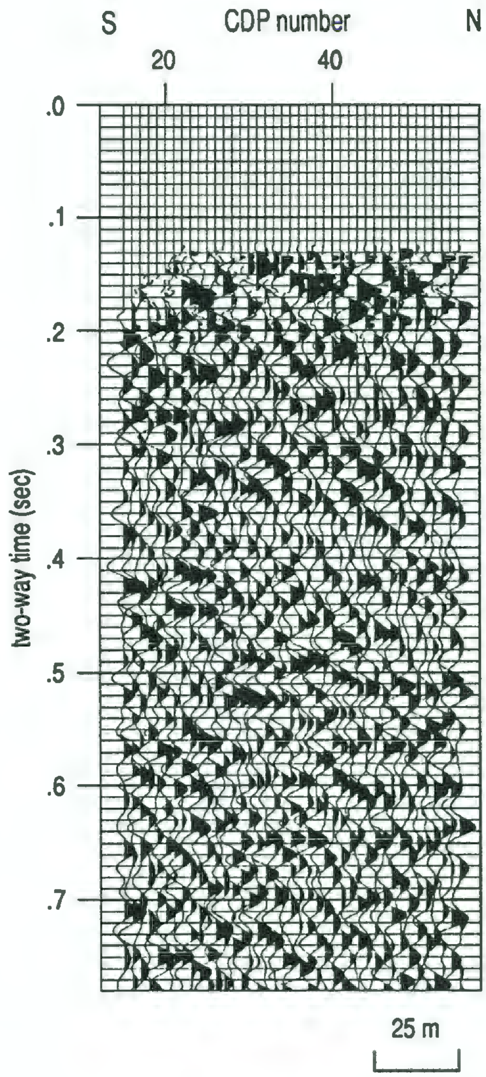

fig 15

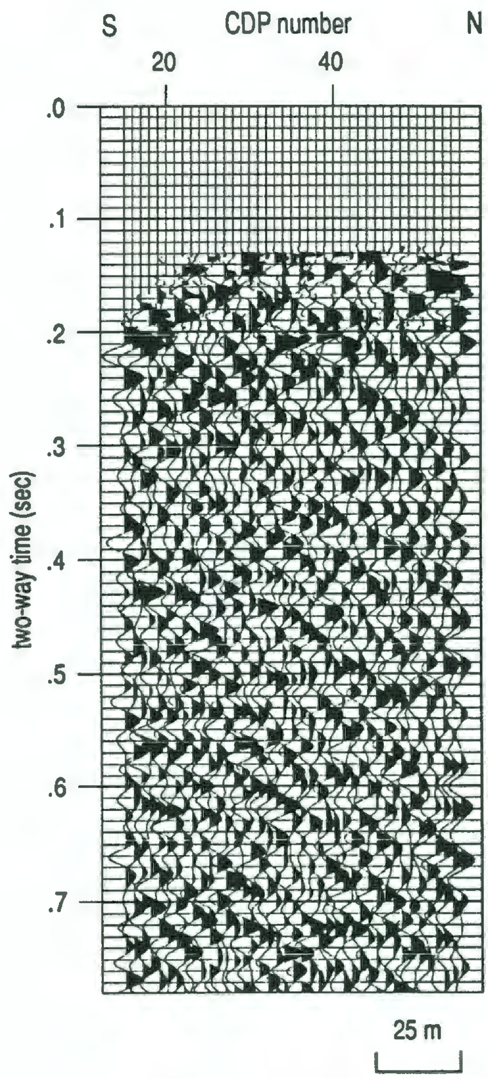

fig 16

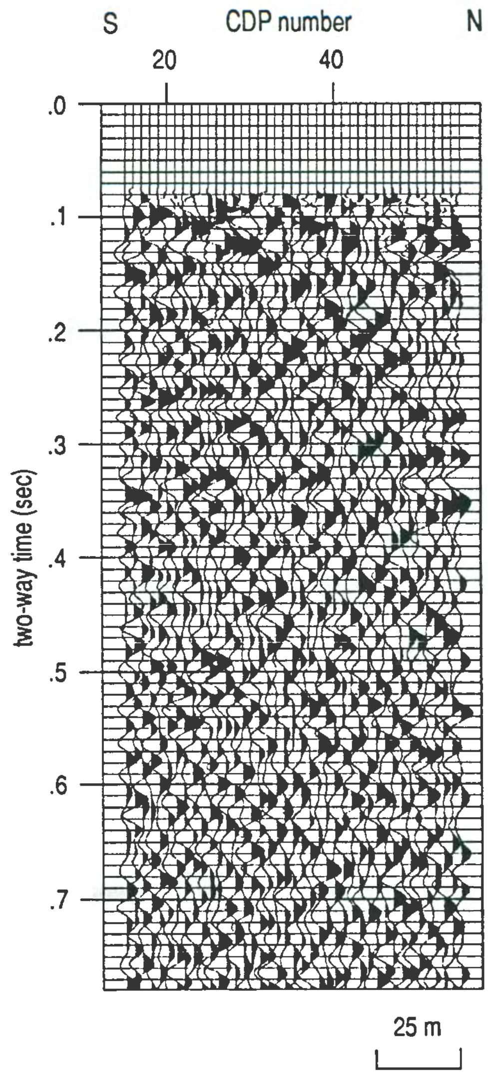

fig 17

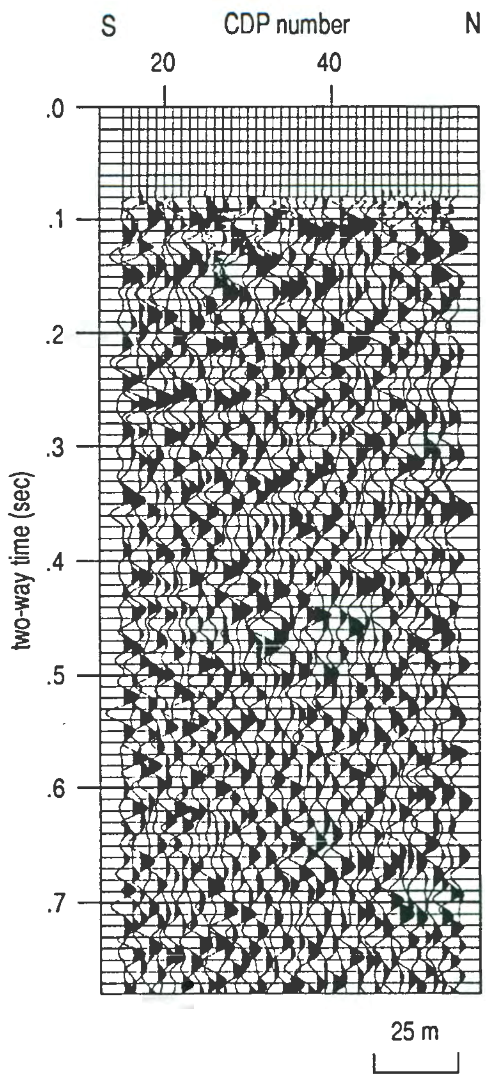

fig 18

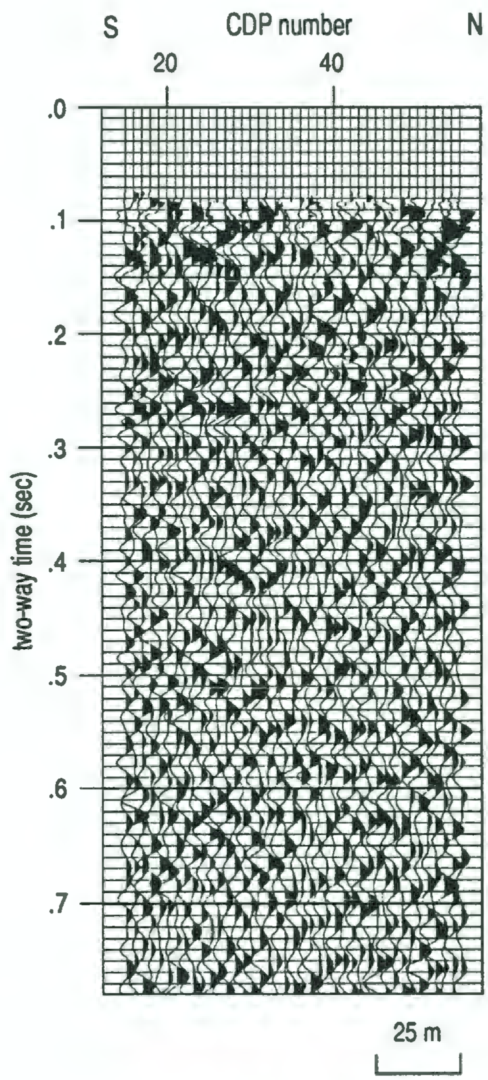

fig 19

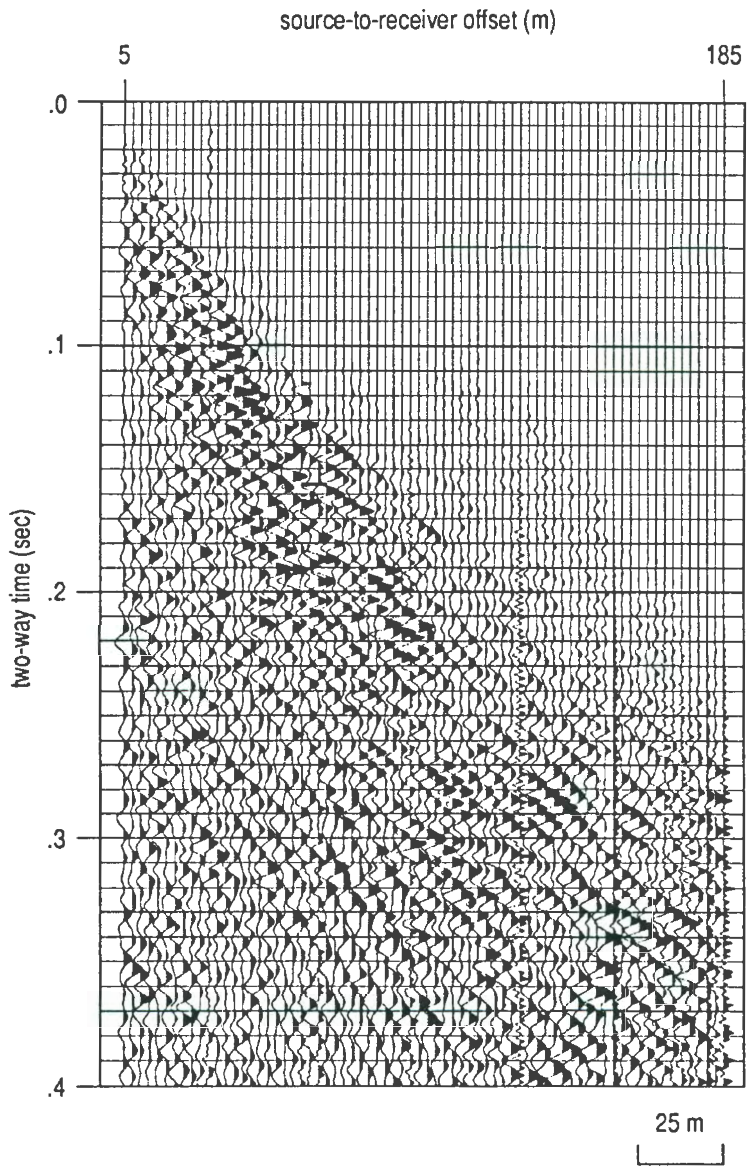

fig 20

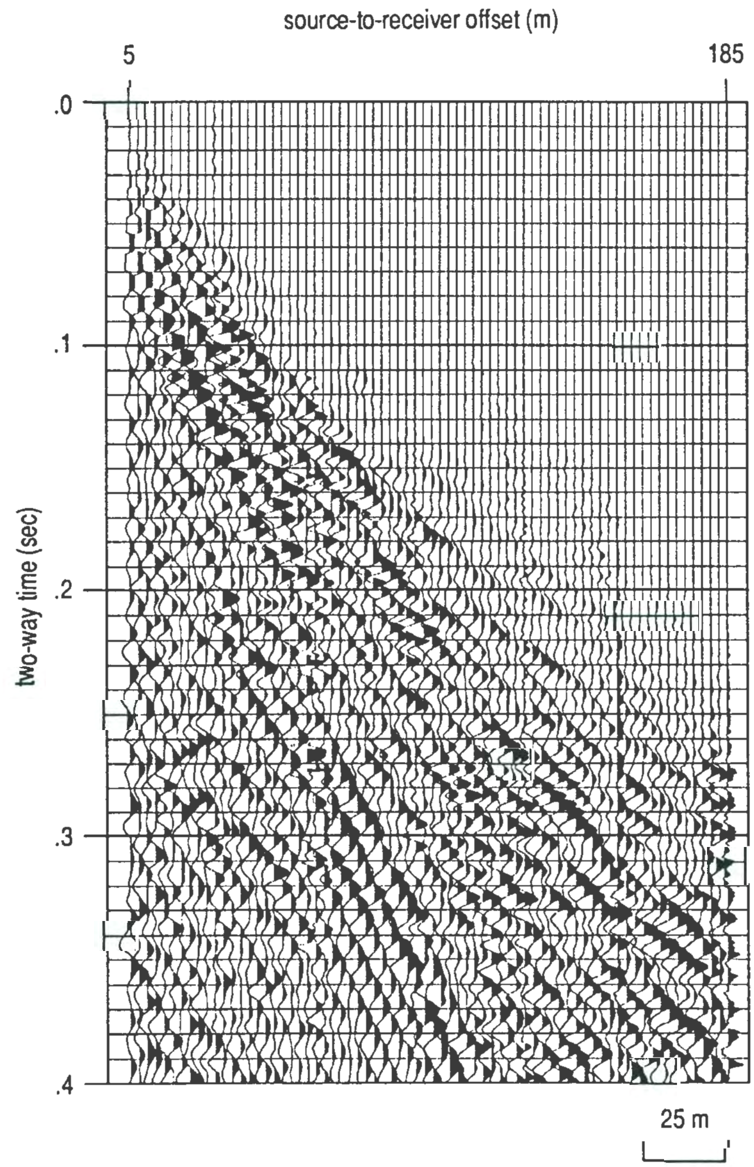

fig 21

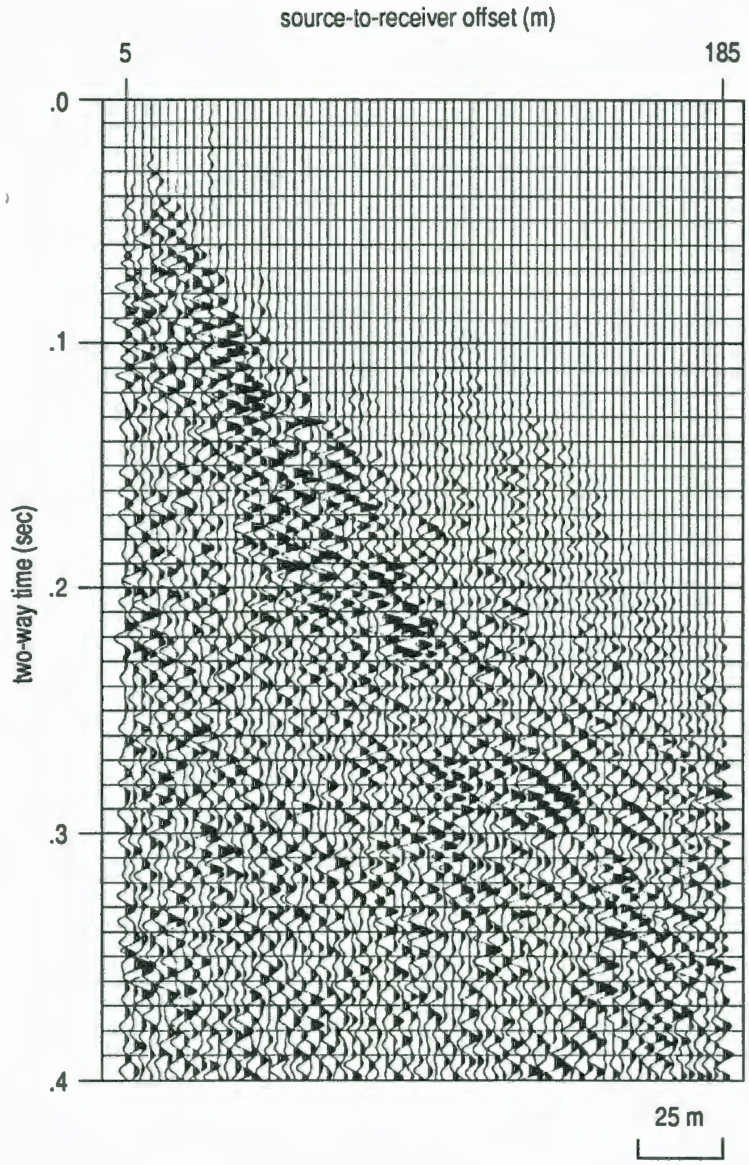

fig 22

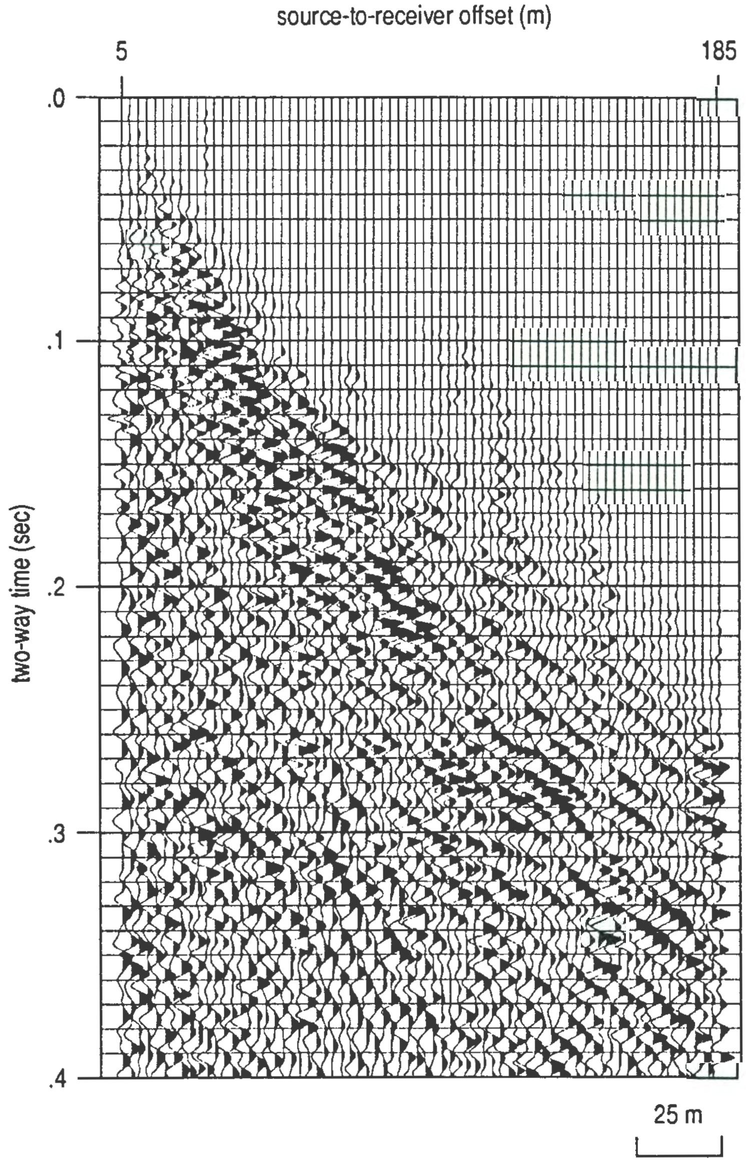

fig 23